

## Taguchi-Based Optimization of Tig Welding for Joining Low-Carbon Steel (ST 37) and Stainless Steel (SUS 304)

Akhmad Kusnadi<sup>1</sup>, Khoirudin<sup>1\*</sup>, Karyadi<sup>1</sup>, Amir<sup>1</sup>, Muhamad Taufik Ulhakim<sup>1</sup>, Amri abduh<sup>2</sup>, Agus Hananto<sup>3</sup>

<sup>1</sup>Department of Mechanical Engineering, Faculty of Engineering, Universitas Buana Perjuangan Karawang, Jl. Ronggo Waluyo Sirnabaya, Karawang 41361, West Java, Indonesia.

<sup>2</sup>Department of Mechanical Engineering, Sekolah Tinggi Teknologi Wastukencana, Jl. Cikopak No.53, Purwakarta, West Java, 41151, Indonesia.

<sup>3</sup>Department of Informatic Engineering, Faculty of Engineering Technology, Asia E University, Subang Jaya, 47500, Selangor, Malaysia.

### ABSTRACT

This study investigates the optimization of tungsten inert gas (TIG) welding parameters for joining dissimilar metals, specifically ST37 low-carbon steel and SUS 304 stainless steel, using the Taguchi L9 experimental design. The welding parameters evaluated include welding current (45-65 A), tungsten electrode diameter (1.6-2.4 mm), and shielding gas flow rate (12-18 LPM). The aim is to enhance joint integrity and mechanical properties by systematically analyzing the influence of these parameters on hardness and tensile load (TS loads). Hardness testing revealed that the weld zone exhibited the highest hardness, followed by the heat-affected zone and base metal. Tensile testing showed that the highest TS loads of 341 kgf were achieved at 45 A, 1.6 mm electrode diameter, and 12 LPM gas flow rate. Signal-to-noise ratio analysis and analysis of variance (ANOVA) indicated that welding current had the most significant influence on hardness and TS loads, with contributions of 39% and 41.27%, respectively, followed by electrode diameter (17% and 36.42%). In comparison, the gas flow rate had the least impact (45% and 22.31%). However, ANOVA results showed that none of the factors exhibited statistical significance ( $P > 0.05$ ). The findings contribute to the field of welding engineering by providing optimized TIG welding parameters for ST37-SUS 304 joints, enhancing their reliability in various industrial applications such as automotive manufacturing, oil and gas, and power generation, where durable and corrosion-resistant welds are crucial.

#### Article information:

Submitted: 30/01/2025

Revised: 12/02/2025

Accepted: 13/02/2025

Published: 15/02/2025

#### Author correspondence:

\* ✉:

[khoirudin@ubpkarawang.ac.id](mailto:khoirudin@ubpkarawang.ac.id)

#### Type of article:

Research papers

Review papers

This is an open access article under the [CC BY-NC](https://creativecommons.org/licenses/by-nc/4.0/) license

**Keywords:** TIG Welding, Hardness test, Tensile loads, ST 37, SUS 304



### 1. Introduction

The fusion of dissimilar metals, particularly low-carbon metals and stainless steel, is crucial in diverse industrial sectors. This welding methodology is essential for automotive manufacturing, shipbuilding, petroleum and natural gas extraction, power generation, aerospace technology and food production. These industries often utilize the combined properties of both materials: low-carbon steel for cost-effectiveness and mechanical strength, and stainless steel for superior corrosion resistance and durability of the final product. However, differences in thermal expansion, melting points, and metallurgical compatibility pose challenges in achieving strong, defect-free welds. Optimizing tungsten inert gas (TIG) welding parameters for joining dissimilar metal joints is essential for enhancing weld strength, structural integrity, and long-term performance. In automotive manufacturing, reliable welding of exhaust systems and chassis components ensures safety and durability, whereas in the oil and gas sector, practical welding of pipelines and pressure vessels prevents failure under extreme conditions. Similarly, power plants rely on robust welded joints in heat exchangers and boilers to withstand high-temperature

and corrosive environments. Addressing these challenges using advanced welding techniques improves the efficiency, reliability, and effectiveness of industrial applications, making this study highly relevant for engineering and manufacturing innovations. Technological advances have rendered welding indispensable for industrial development. Metal joining connects two or more metal parts, both homogeneous and heterogeneous [1]. High-quality welds are essential to ensure robust, secure, and durable construction [2]. The quality of welded joints and adherence to construction standards, particularly in the oil and gas industry, such as in pipeline installations, are significantly influenced by the strength of the welded joints [3]. Welding processes in the manufacturing industry frequently involve dissimilar metals, such as stainless steel and low-carbon steel [4].

The strength and integrity of welded joints are critical factors in ensuring structural safety and material performance. The process of joining dissimilar metals is complex owing to the significant differences in the thermal conductivity of each metal [5]. Various methodologies have been developed to enhance the welding quality of materials. Baskutis *et al.* [6] conducted a study utilizing different types of stainless steels (AISI 304, 314, 316L, and 420) and S355MC steel to evaluate their weldability. Nurcholis *et al.* [7], conducted welding of SUS 304 and SS 400 materials using different welding positions (1G, 2G, and 3G). Visual inspection confirmed the absence of any weld defects. The hardness test results indicated that the highest hardness value was observed in the weld metal at the 3G position, whereas the 2G position exhibited the lowest hardness value. Haribabu *et al.* [8] employed AISI 304 austenitic stainless steel round bar and D3 tool steel with a diameter of 16 mm and a length of 80 mm for friction welding joints. The welded samples were sectioned crosswise to prepare metallographic specimens and hardness measurements.

TIG welding with current variations of 40-60 A utilizing AISI 304 was conducted by Cahyono *et al.* [9], who demonstrated that when employing a current of 60 A in the TIG welding process, the resulting welded joints exhibited optimal penetration with no visible gaps between the plates. However, when currents of 40 and 50 A were used, the weld joint was not clearly visible, and a gap remained between the plates. Khalim [10] investigated TIG welding with respect to the shielding gas flow rate using Al-5083 and AL-6061 and indicated that after comparing all the data at a gas flow rate of 15 LPM, the average TS-load recorded was 168.29 MPa. Furthermore, the hardness increased significantly, particularly in the weld metal area, reaching 76 HVN. The effect of TIG welding with variations in the electrode diameter was examined using AISI 1050 by Rosidah *et al.* [11]. The resulting hardness test yielded the highest hardness value of 41.125 HRC with a diameter variation of 2.4 mm and a welding speed of 2 mm/s. Mulyadi *et al.* [12] reported TIG welding on SUS 304 stainless steel with the parameters of welding current, gas flow, and electrode diameter. The results showed that The highest TS load achieved was 1393.00 kgf, and there was a decrease in hardness from the weld zone to the base metal.

Based on several existing studies, this study utilized ST 37 and SUS 304 materials with TIG welding. TIG welding is a welding process that employs an electric arc formed between a nondissolved tungsten electrode and the work material, with a shielding gas used to prevent contamination and oxidation of the weld zone [13-15]. TIG welding is employed to produce high-quality welded joints and is one of the most widely used welding methods in the manufacturing industry [16-18]. The welding parameters were determined using the Taguchi L9 experimental-design matrix. The welding results were subjected to hardness and tensile tests. Based on the results of this study, the optimal parameters for welding different materials (ST 37 and SUS 304) using TIG welding were determined.

Despite extensive research on dissimilar metal welding, challenges persist in optimizing the process parameters to achieve defect-free, high-strength joints between low-carbon steel (ST37, classified as S235JR under EN 10025-2 [19], A283 [20], Grade C/A36 [21] in ASTM, and SS400 in JIS G3101 [22]) and stainless steel (SUS 304, standardized as X5CrNi18-10 in EN 10088-1 [23], AISI 304 in ASTM A240 [24]/A276 [25], and 1.4301 in DIN 17440 [26]) owing to differences in their thermal expansion, melting points, and metallurgical compatibility. Although existing studies have focused on various welding techniques, limited research has explored the systematic optimization of TIG welding parameters for these

materials. This study addresses this gap by employing the Taguchi L9 experimental design to optimize the welding current, shielding gas flow rate, and welding speed to ensure enhanced joint integrity. Mechanical characterization through hardness and tensile tests provides insights into the weld strength and performance. The novelty of this study lies in its integrated approach to parameter optimization, which aims to minimize brittle intermetallic formation while maximizing mechanical strength. These findings are expected to contribute to the field of welding engineering by providing optimized TIG welding parameters for ST37-SUS 304 joints, thereby enhancing their reliability in industries such as oil and gas, automotive, and power generation, where durable and corrosion-resistant welds are crucial.

## 2. Methods

### 2.1. Materials

TIG welding was used to join ST37 (S235JR, A36) and SUS 304 (X5CrNi18-10, AISI 304) sheets with a thickness of 1 mm, employing ER309L (AWS A5.9 [27]/ EN ISO 14343-A: W 23 12 L [28]) as the filler metal. Welding dissimilar metals with such thin dimensions requires precise control of the heat input to prevent burn-through and excessive warping of the base metal. Direct Current Electrode Negative (DCEN) polarity was selected, as illustrated in Figure 1, with thoriated tungsten electrodes of 1.6, 2.0, and 2.4-mm diameters to ensure arc stability. The TIG welding current ranged between 45 and 65 A, whereas the shielding gas flow rate varied from 12 to 18 LPM, providing adequate protection against oxidation. To minimize the heat input and distortion, a stringer-bead technique with a high travel speed ( $\geq 250$  mm/min) was employed, allowing for uniform weld deposition.

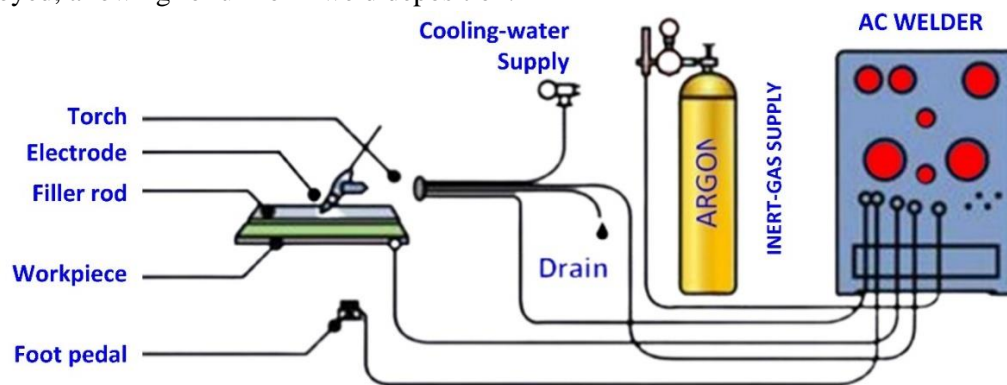


**Figure 1.** Schematic of the TIG-welding machine.

Single-pass welding without weaving was performed using multiple tack welds to maintain sheet alignment and reduce residual stresses. The interphase temperature was maintained below 100 °C to limit heat accumulation and prevent the formation of metallurgical defects. Complete penetration without burn-through was achieved using precise parameter control, which eliminated the need for a backing plate. In this study, the TIG welding parameters for ST37-SUS 304 dissimilar joints were systematically optimized, resulting in defect-free high-strength welds with minimal intermetallic formation.

#### 2.1.1. Filler ER309L

The filler material ER309L (AWS A5.9 [27]/ EN ISO 14343-A: W 23 12 L [28]) was selected for joining ST37 and SUS 304 owing to its exceptional metallurgical compatibility, mechanical properties, and corrosion resistance. Its high chromium (23%) and nickel (12%) contents contribute to the formation of a stable austenitic microstructure, which reduces the likelihood of brittle intermetallic phases in the fusion zone and minimizes cracking caused by disparities in the thermal expansion coefficients and melting points of the base metals. Furthermore, ER309L inhibits excessive carbon migration from ST37 to the weld, thereby reducing carbide precipitation and intergranular corrosion while maintaining high toughness and ductility. These characteristics are crucial for applications exposed to cyclic loads and thermal stresses, such as those in the oil and gas, automotive, and power generation sectors. The low-carbon variant enhances corrosion

resistance by limiting chromium carbide precipitation, preventing weld decay, and extending the lifespan of the joint in humid and high-temperature environments. As a widely recognized filler for dissimilar metal welding, ER309L has shown consistent performance in the TIG, MIG, and SMAW processes, making it an ideal choice for producing defect-free, high-strength, and long-lasting welds in ST37-SUS 304 joints.

### 2.1.2. Base metal – dissimilar materials

This study focuses on two widely used industrial materials: ST37 low-carbon steel, which conforms to DIN 17100 [29], and SUS 304 stainless steel, which conforms to the ASTM A240 standard [24]. These materials were selected owing to their extensive applications in the construction and manufacturing industries and their contrasting mechanical and chemical properties. To ensure uniformity in mechanical testing, the test specimens were prepared with a consistent thickness of 1 mm, in compliance with ASTM E8 standards [30]. Tensile test specimens were fabricated according to ASTM E8 specifications [30], and their welding configurations are shown in Figure 2.

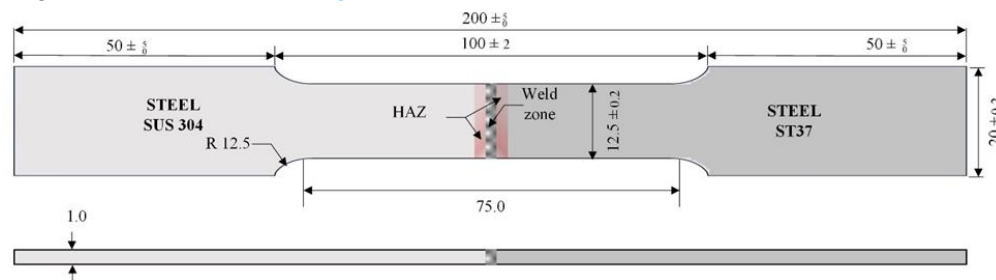


**Figure 2.** Schematic of TIG-welded ST37 and SUS 304.

ST37 low-carbon steel is frequently employed in structural applications because of its favorable combination of strength, ductility, and weldability, making it an economical choice for engineering applications. In contrast, SUS 304 austenitic stainless steel is highly regarded because of its superior corrosion resistance, high strength, and excellent mechanical properties, which make it particularly suitable for harsh environments and demanding operational conditions. The chemical compositions and mechanical properties of ST37, SUS 304, and ER309L are summarized in Table 1 and Table 2, respectively.

**Table 1.** Chemical compositions ST 37, SUS 304 (ASTM A240) and Filler ER309L

Materials	C	Si	Mn	P	S	Cu	Cr	Ni	N
ST 37 [31]*	0.12	0.10	0.50	0.04	0.05	0.10	-	-	-
SUS 304 [32]	0.02	0.67	1.78	0.03	0.04	-	18.11	8.01	0.06
Filler ER309L [27]	≤0.03	0.30-0.65	1.0-2.5	≤0.03	≤0.03	≤0.75	23.0-25.0	12.0-14.0	-

\*) Aluminum, Al = 0.02

**Table 2.** Mechanical Properties of ST37 (DIN 17100), SUS 304 (ASTM A240) and Filler ER309L (AWS A5.9)

Materials	Yield strength (MPa)	Tensile test load (MPa)	Elongation (%)	Hardness (HRC)	Elastic modulus (GPa)
ST 37 [31]	≥ 235	300–510	≥ 18	120–180	200
SUS 304 [32]	≥ 205	≥ 515	≥ 40	≤ 92	193
Filler ER309L [27]	-	≥ 520	≥ 30	-	-

## 2.2. Taguchi experimental design

This study employed the Taguchi method to optimize the welding parameters for joining dissimilar metals, specifically, ST37 low-carbon steel and SUS 304 stainless steel. The objective was to enhance joint integrity by systematically analyzing key welding variables. The experimental design incorporated three factors at three levels: the electric current, tungsten electrode diameter, and gas flow rate. By utilizing the

Taguchi L9 orthogonal array, this study aimed to identify the optimal parameter combinations that would result in improved welding performance and mechanical properties of the dissimilar joints [33].

A detailed summary of the Taguchi L9 experimental design, including the three variables and their respective levels, is listed in Table 3. This table outlines the structured experimental approach used to evaluate the impact of each parameter on the weld quality, ensuring a robust and statistically sound optimization process. The implementation of this methodology facilitates a more efficient and reliable welding process, minimizes variability, and enhances the reproducibility.

**Table 3.** Taguchi experimental design

Code	Parameter	Level		
		I	II	III
A	Electric current (A)	45	55	65
B	Tungsten electrode diameter (mm)	1.6	2.0	2.4
C	Gas flow rate (LPM)	12	15	18

Table 4 provides a comprehensive overview of the L9 orthogonal array, detailing the parameter combinations used in the nine experimental runs. Each run produced three samples, resulting in 27 welded specimens. This structured experimental approach ensured a statistically robust evaluation of the welding performance, allowing for optimized parameter selection that enhanced the integrity and mechanical strength of dissimilar metal joints.

**Table 4.** The matrix Taguchi experimental design

Run. No.	Parameter code			Tensile test load			The hardness test		
	A	B	C	TS1	TS2	TS3	H1	H2	H33
1	1	1	1	TS1-1	TS2-1	TS3-1	H1-1	H2-1	H3-1
2	1	2	2	TS1-2	TS2-2	TS3-2	H1-2	H2-2	H3-2
3	1	3	3	TS1-3	TS2-3	TS3-3	H1-3	H2-3	H3-3
4	2	1	2	TS1-4	TS2-4	TS3-4	H1-4	H2-4	H3-4
5	2	2	3	TS1-5	TS2-5	TS3-5	H1-5	H2-5	H3-5
6	2	3	1	TS1-6	TS2-6	TS3-6	H1-6	H2-6	H3-6
7	3	1	3	TS1-7	TS2-7	TS3-7	H1-7	H2-7	H3-7
8	3	2	1	TS1-8	TS2-8	TS3-8	H1-8	H2-8	H3-8
9	3	3	2	TS1-9	TS2-9	TS3-9	H1-9	H2-9	H3-9

### 2.3. Hardness testing

Hardness testing was conducted using a Portable Hardness Tester that was calibrated prior to the measurement to ensure accuracy and consistency. The calibration process involved testing the instrument on a standard reference block with known hardness. Multiple measurements were taken at different points on the block to verify precision. If discrepancies were observed, adjustments were made until the readings aligned with the standard reference values. Hardness measurements were performed on the prepared samples using a standardized procedure to minimize variability. Five indentations were made on each sample, ensuring adequate spacing between the measurement points to avoid interference. The average hardness was calculated from these measurements to provide a representative assessment of the material hardness.

Figure 3 shows the hardness measurements taken at five locations: two points on ST37 steel (2 mm and 10 mm from the weld center), two points on SUS 304 stainless steel (2 mm and 10 mm from the weld center), and one point in the weld zone (WZ). The 2 mm points represent the heat-affected zone (HAZ), whereas the 10 mm points correspond to the base metal (BM). The hardness values were recorded directly from the instrument and analyzed to assess the distribution across the welded joints. The results summarized in Table 5 show significant variations in hardness. The weld zone exhibited the highest hardness, followed by the heat-affected zones of ST37 and SUS 304. In contrast, the base metals had lower hardness values than their respective heat-affected zones, indicating the influence of welding on the microstructure and

mechanical properties of the material.

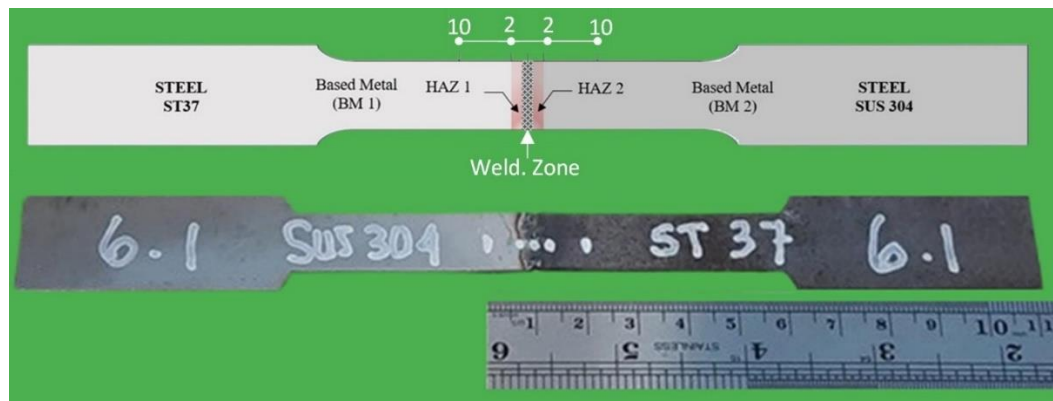


**Figure 3.** Positions of hardness measurements across the weldment: weld zone (WZ), heat-affected zone (HAZ), and base metal (BM)

**Table 5.** Average hardness of three samples for each run number

Run. No.	Current (A)	Electrode diameter (mm)	Gas flow rate (LPM)	The average hardness (HRC)				
				WZ-10 mm	WZ-2 mm	WZ	WZ+2 mm	WZ+10 mm
1	45	1.6	12	29.20	44.66	52.16	39.30	27.03
2	45	2.0	15	29.46	44.63	55.30	41.40	39.93
3	45	2.4	18	35.33	44.26	51.60	44.06	37.86
4	55	1.6	15	34.60	43.96	54.76	41.73	36.13
5	55	2.0	18	37.56	45.40	59.53	42.23	39.20
6	55	2.4	12	35.50	46.30	59.56	51.90	47.70
7	65	1.6	18	41.30	49.96	60.80	54.30	45.03
8	65	2.0	12	40.73	48.70	61.23	48.53	41.80
9	65	2.4	15	44.26	54.20	63.16	54.06	46.56

#### 2.4. Tensile load

Tensile load tests were conducted using a Hung Ta HT-9102 universal testing machine with a maximum load capacity of 50 kN and an operating voltage of 380 V. This test was performed according to the ASTM E8 standards [30] to evaluate the TS-load and elongation of welded specimens. The specimen was securely clamped between the upper and lower grips of the machine to ensure proper alignment and to prevent slippage during testing. A uniaxial tensile force ( $F$ ) was applied gradually in the opposite directions of the top and bottom grips at a constant crosshead speed of 30 mm/min until the specimen was fractured. The applied force and elongation were continuously recorded to analyze the mechanical properties of welded joints. The tensile test setup is shown in Figure 4.

#### 2.5. Signal-to-noise ratio (S/N ratios)

The signal-to-noise (S/N) ratios were used to evaluate the sensitivity of the input factors and to optimize the welding parameters by minimizing variations in the response variables. In Taguchi analysis, the response characteristics are categorized into three types: (1) larger-the-better, used to maximize the desired responses, such as the TS-load; (2) smaller-the-better, applied when minimizing defects or errors, such as porosity or distortion; and (3) nominal-the-best, utilized when targeting a specific value, such as dimensional accuracy. By calculating the S/N ratios, the influence of each factor on the welding performance can be systematically analyzed, aiding in the selection of optimal parameter combinations to achieve high-quality welds with improved mechanical properties. Equations (1)– (3) [34, 35].

Smaller is better

$$\frac{S}{N} = -10 \text{Log}10 \sum_{i=1}^{n_0} \frac{y_i^2}{n_0} \quad (1)$$

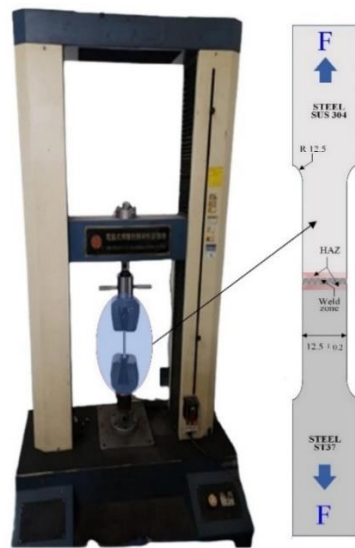


**Figure 4.** Tensile Testing Equipment for ST37 and SUS 304

Larger is better

$$\frac{s}{N} = -10 \text{Log}_{10} \frac{1}{n_0} \sum_{i=1}^{n_0} \frac{1}{y_i^2} \tag{2}$$

Nominal is the best

$$\frac{s}{N} = -10 \text{Log}_{10} \frac{\bar{y}^2}{s^2} \tag{3}$$

where  $\bar{y}$  represents the average value of the data and  $s$  is the standard deviation. Because the characteristics of the TS-load and hardness tests generally indicate that higher values correspond to improved material performance, the Taguchi analysis in this study was designed using the 'Larger-the-Better' criterion.

### 3. Results and Discussion

#### 3.1 Hardness testing result

Figure 5 illustrates the hardness test results, revealing that the hardness values were generally higher in regions closer to the weld. In samples  $A_1B_3C_3$  and  $A_2B_2C_3$ , the hardness measured at 2 mm from the weld was significantly greater than that at 10 mm, indicating that rapid cooling near the weld zone led to localized hardening within the heat-affected zone (HAZ). This phenomenon is attributed to the thermal gradient and phase transformations that occur during welding.

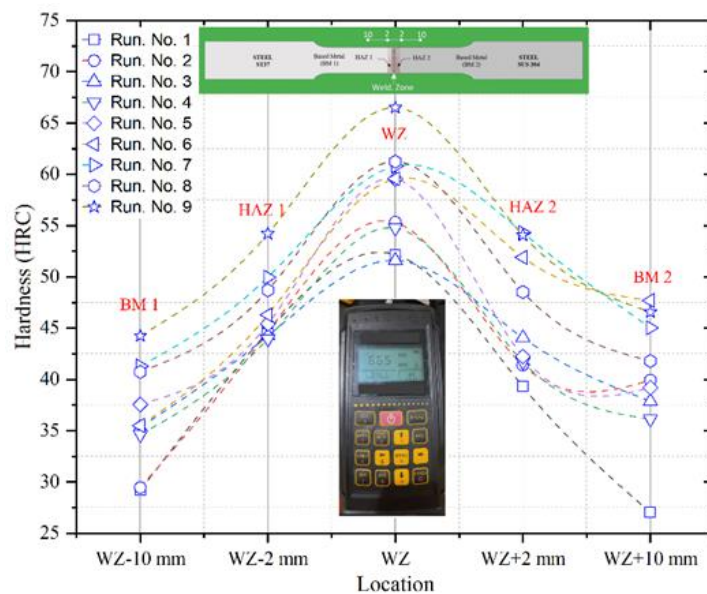


**Figure 5.** Hardness distribution in TIG-Welded Joints

Furthermore, the weld center, particularly in samples  $A_2B_3C_2$ , exhibited the highest hardness value of 60 HRC, followed by the heat-affected zone (HAZ) with a maximum hardness of 52 HRC, and the base metal (BM), which recorded the lowest hardness of 45 HRC. The hardness trend ( $WZ > HAZ > BM$ ) can be explained by the metallurgical transformations influenced by thermal exposure. The weld zone (WZ) undergoes rapid melting and solidification, leading to finer microstructures and possible martensitic or dendritic phase formation, resulting in maximum hardness. The heat-affected zone (HAZ) experiences thermal cycles that alter the grain structure, causing partial recrystallization and hardening, although not as intensely as the WZ. In contrast, the base metal (BM) remained unaffected by thermal alterations, retaining its original microstructure and exhibiting the lowest hardness. These findings are in agreement with those of Mulyadi *et al.* [12], who similarly observed the  $WZ > HAZ > BM$  hardness trend in TIG-welded dissimilar joints owing to phase transformations and thermal effects. These results emphasize the critical role of optimizing welding parameters to achieve a uniform hardness distribution, enhance structural integrity, and minimize defects in TIG-welded ST37-SUS 304 dissimilar joints.

### 3.2 Tensile test load analysis

Figure 6 shows the tensile test results of the TIG-welded samples under varying welding currents, tungsten electrode diameters, and gas flow rates. The highest TS-load of 341 kgf was achieved at 45 A, 1.6 mm electrode diameter, and 12 LPM gas flow rate, as illustrated in Figure 7. However, the recorded TS-load values for the three samples under these conditions (341, 179, and 307 kgf) indicate a high standard deviation, suggesting significant variability in the weld quality. Conversely, the lowest TS-load of 141 kgf was observed at 55 A, 2.4 mm electrode diameter, and 18 LPM gas flow rate, with individual TS-load values of 141, 252, and 255 kgf, showing substantial fluctuations. Increasing the welding current beyond 45 A did not necessarily enhance the TS load. A smaller electrode diameter (1.6 mm) and moderate gas flow rate (12 LPM) yielded better tensile performance. The observed variations may be attributed to microstructural changes, including grain coarsening and intermetallic formation, induced by the different welding parameters.

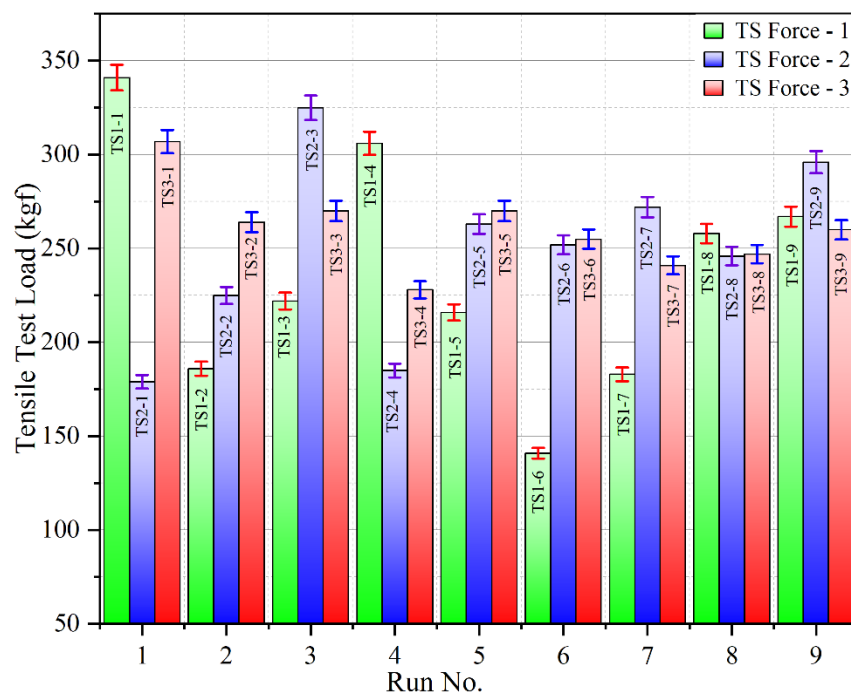


Figure 6. Tensile load results of 27 samples of TIG-welded ST37-SUS 304 joints.

The average TS-load analysis obtained the highest mean TS-load of 275.67 kgf using a 45 A current, 1.6 mm electrode diameter, and 12 LPM gas flow rate. In contrast, the lowest average TS-load of 216.00 kgf resulted from a 55 A current, 2.4 mm electrode diameter, and 18 LPM gas flow rate. These results suggest

that a lower current (45 A), smaller electrode diameter (1.6 mm), and moderate gas flow rate (12 LPM) optimize the TS load performance. The TS-load values aligned with the ST37 material specification reported by [31], but remained lower than the SUS 304 specification in [32]. Additionally, the obtained results fell below the filler metal specifications outlined in [27], suggesting that heat accumulation during the TIG welding of thin materials may have contributed to the reduction in TS loads. This phenomenon is consistent with the findings of Mulyadi *et al.* [12], who observed similar trends in thin-section TIG welding. These insights highlight the necessity of optimizing the welding parameters to enhance the stability and uniformity, thereby ensuring optimal weld quality for industrial applications. Although the highest TS-load configuration is a primary reference, further studies are required to improve the consistency and mechanical reliability of TIG-welded ST37-SUS 304 dissimilar joints.

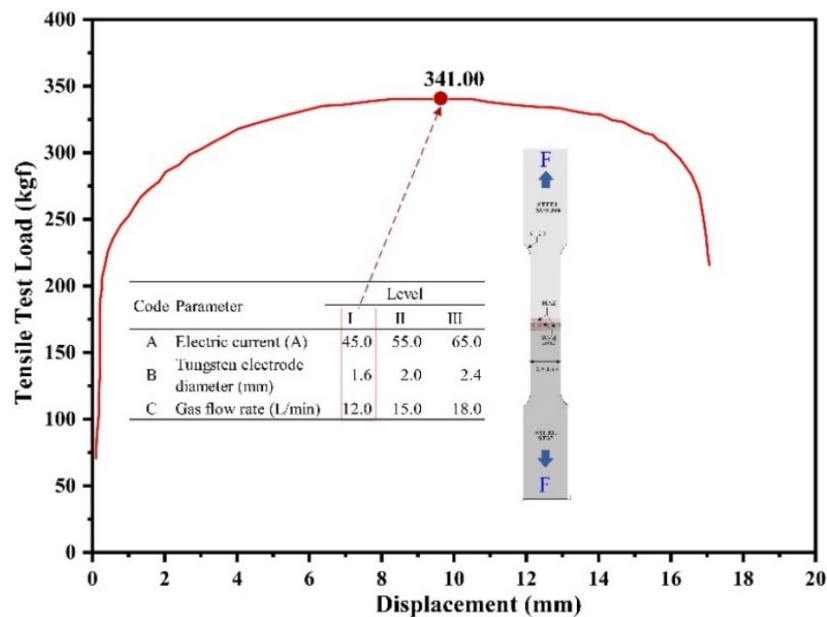


Figure 7. The highest TS-load of the TIG-welded ST37-SUS 304 joints.

### 3.3 S/N ratios analysis

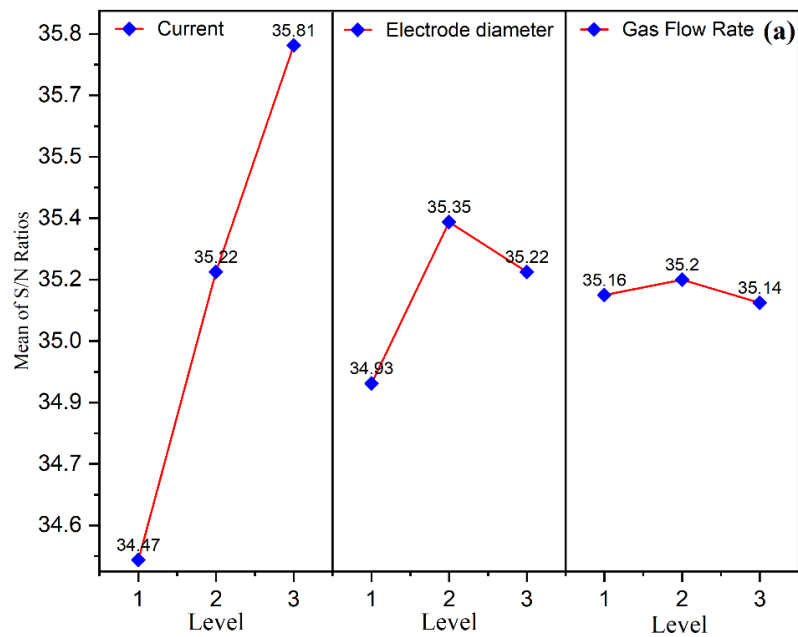
Table 6 presents the S/N ratio analysis based on the 'larger is better' criterion for evaluating the influence of key parameters on the hardness and TS-load performance.

Table 6. Signal-to-noise (S/N) ratio for average TS-load and hardness in the weld zone (WZ).

Level	Ave. Hardness on WZ			Ave. TS-load		
	Ampere	Electrode dia.	Gas flow rate	Ampere	Electrode dia.	Gas flow rate
1	48.18	47.90	47.82	34.47	34.93	35.16
2	47.41	47.65	47.80	35.22	35.35	35.2
3	48.02	48.05	47.99	35.81	35.22	35.14
Delta	0.78	0.40	0.19	1.34	0.42	0.06
Rank	1	2	3	1	2	3

The S/N ratio analysis highlights the critical influence of amperage on the hardness performance, as evidenced by the highest value (1.34) among the evaluated parameters. The highest S/N ratio was observed at Level 1 (35.81), followed by Level 2 (35.22) and Level 3 (34.47), confirming that lower amperage levels contribute more significantly to hardness enhancement.

The electrode diameter also plays a substantial role, with a delta value of 0.42, indicating its secondary influence on the hardness optimization. Conversely, the gas flow rate had the least impact, with a delta value of only 0.19, suggesting a minimal effect on the hardness variation. These results, as shown in Figure 8, reinforce the need to prioritize amperage settings in process optimization to achieve improved hardness. These findings are in line with the study previously reported by Mulyadi *et al.* [12], further validating the influence of amperage on hardness performance.



**Figure 8.** S/N ratios—larger is better—for hardness distribution in TIG-welded joints of ST37 and SUS 304.

For the TS loads (TS-load), a similar trend was observed, where the amperage remained the most dominant factor, exhibiting the highest delta value (0.78). The peak S/N ratio occurred at Level 3 (48.18), followed by Level 1 (48.02) and Level 2 (47.41), indicating that higher amperage settings enhanced the TS-load performance. The electrode diameter also had a notable impact, with a delta value of 0.40, reinforcing its role in mechanical strength enhancement. In contrast, the gas flow rate remained the least influential parameter, yielding a delta value of only 0.06, confirming its negligible effect on the TS-load variation.

As depicted in [Figure 9](#), these findings suggest that optimizing the amperage should be the primary focus for enhancing the TS load, whereas electrode diameter adjustments can serve as a secondary optimization strategy. These results are consistent with those of a study previously reported by Mulyadi *et al.* [12], further supporting the critical role of amperage in TS load improvement.

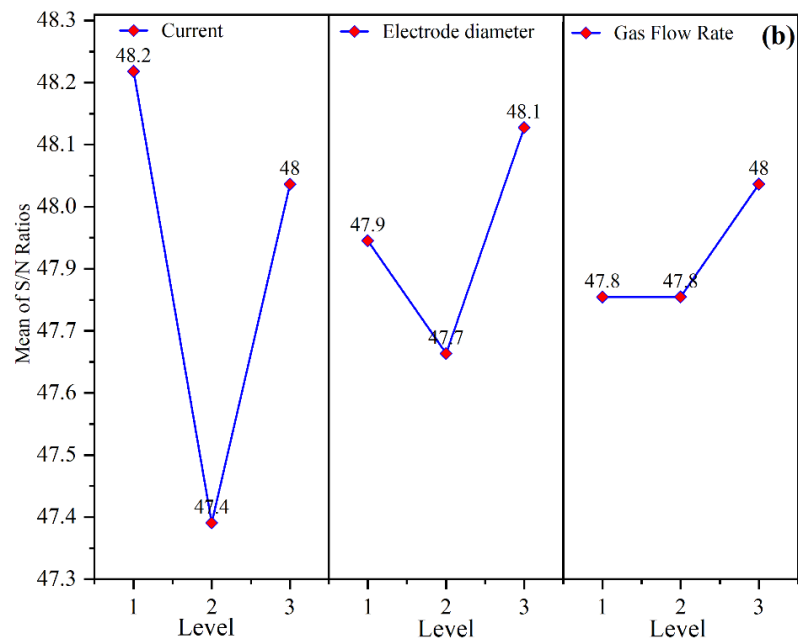


**Figure 9.** S/N ratios—larger is better—for TS-load in TIG-welded joints of ST37 and SUS 304.

### 3.4. Analysis of variance (ANOVA)

Table 7 presents the contribution of each factor to the tensile test results, highlighting that the welding current has the most significant influence (41.27%) on the hardness and TS-load, followed by the tungsten electrode diameter (36.42%), while the gas flow rate has the least impact (22.31%). These findings suggest that the welding current and electrode diameter are the primary factors to be considered for process optimization.

The ANOVA results indicated that none of the evaluated factors exhibited statistical significance, as evidenced by P-values exceeding 0.05. Despite this, the contribution analysis provides valuable insights into the relative influence of each of these parameters. For hardness, the gas flow rate contributed the most (45%), followed by the welding current (39%) and electrode diameter (17%). However, the F-values remained low ( $\leq 0.51$ ), confirming that these variations were not statistically significant.

Similarly, for the TS-load, the welding current exhibited the highest contribution (41.27%), followed by the electrode diameter (36.42%) and gas flow rate (22.31%). Again, the F-values ( $\leq 0.06$ ) and high P-values ( $\geq 0.819$ ) indicate that these effects are not statistically significant.

**Table 7.** Analysis of Variance

Statistic and contributions	Hardness parameter			TS loads parameters		
	Weld. current	Electrode Dia.	Gas Flow Rate	Weld. current	Electrode Dia.	Gas Flow Rate
DF	1	1	1	2	2	2
Adj SS	5.496	2.381	6.344	44.44	39.22	24
Adj MS	2.748	1.19	3.172	44.44	39.22	24
F-Value	0.45	0.19	0.51	0.06	0.05	0.03
P-Value	0.692	0.838	0.66	0.819	0.83	0.866
Contributions (%)	39	17	45	41.27	36.42	22.31

These results align with those of previous studies by Mulyadi *et al.* [12] and Basit *et al.* (2024) [36], who also reported no statistically significant influence of welding current, electrode diameter, and gas flow rate on mechanical properties under similar experimental conditions. However, given the higher contributions of welding current and gas flow rate, further experiments or alternative statistical approaches, such as regression analysis, may be necessary to confirm their actual impact on hardness and TS-load optimization.

## 4. Conclusions

This study focuses on optimizing the TIG welding parameters for joining dissimilar metals, specifically ST37 low-carbon steel and SUS 304 stainless steel, using the Taguchi L9 experimental design. The investigated welding parameters included the welding current, tungsten electrode diameter, and shielding gas flow rate, with the primary objective of enhancing the joint integrity and mechanical properties by systematically analyzing their influence on the hardness and tensile strength.

- TIG welding was used to join the ST37 low-carbon steel and SUS 304 stainless steel sheets.
- Hardness testing revealed that the weld zone had the highest hardness, followed by the heat-affected zone (HAZ) and base metal.
- The highest TS load was achieved at 45 A, 1.6 mm electrode diameter, and 12 LPM gas flow rate.
- Welding current had the most significant influence on the hardness and TS loads.
- The electrode diameter had the second most significant influence, whereas the gas flow rate had the least impact.
- The findings provide optimized TIG welding parameters for ST37-SUS 304 joints.
- The optimized parameters enhanced the reliability of the ST37-SUS 304 joints in various industrial applications.

The S/N ratio analysis and ANOVA results confirmed the hierarchy of influence among the welding parameters. These findings provide valuable insights into the optimization of TIG welding parameters, contributing to improved mechanical performance and reliability in various industrial applications.

### Author's Declaration

#### Authors' contributions and responsibilities

**Akhmad Kurnadi** was responsible for data collection, conducting the investigation, and drafting the original manuscript. **Khoirudin** supervised the study and validated the data. **Karyadi** contributed to writing, reviewing, and editing the manuscript, as well as providing supervision, developing the methodology, and conceptualizing the study. Amir assisted with data collection, and **Muhamad Taufik Uihakim** contributed to data analysis. **Amri Abdulah** contributed to TS-load testing and analysis, and **Agus Hananto** was responsible for statistical analysis and data validation.

### Acknowledgment

The authors express their sincere gratitude to the Energy Conversion Laboratory and Mechatronics Laboratory of Universitas Buana Perjuangan Karawang for their valuable support, technical assistance, and access to research facilities during this study. Their contributions were crucial for facilitating the experimental setup, data acquisition and analysis. The authors acknowledge the guidance and constructive feedback provided by their colleagues and faculty members, which significantly enhanced the quality of this study. Finally, the authors extend their appreciation to all individuals and institutions who contributed directly or indirectly to the successful completion of this study.

### Availability of data and materials

All data generated, analyzed, and used to support the findings of this study are available from the corresponding author upon reasonable request. This includes raw, processed, and supplementary materials relevant to this research. Access to data may be granted for academic and research purposes, subject to institutional and ethical guidelines..

### Competing interests

The authors declare no competing or conflicting interests related to this study.

### REFERENCES

- [1] A. Aditia, N. Nurdin, and A. S. Ismy, Analisa kekuatan sambungan material AISI 1050 dengan ASTM A36 dengan variasi arus pada proses pengelasan SMAW, 1 (2019) 1-4.
- [2] G. Gundara and A. A. Biggunah, Analisis Kekuatan Arus Terhadap Ketangguhan dan Ketahanan Sambungan Pada Proses Las Tig, 1 (2021) 233-248.
- [3] R. Rinaldi and R. Usman, Studi eksperimental kekuatan tarik dan kekerasan pada sambungan pipa ASTM A 106 Grade B dengan pengelasan SMAW, 1 (2019) 36-42.
- [4] B. T. Baroto and P. H. Sudargo, Pengaruh arus listrik dan filler pengelasan logam berbeda baja karbon rendah (st 37) dengan baja tahan karat (aisi 316l) terhadap sifat mekanis dan struktur mikro, (2017) 637-642.
- [5] B. N. Güzey and G. İrsel, Investigation of mechanical and microstructural properties in joining dissimilar P355GH and stainless 316L steels by TIG welding process, 205 (2023) 104965.
- [6] S. Baskutis, J. Baskutiene, R. Bendikiene, A. Ciuplys, and K. Dutkus, Comparative research of microstructure and mechanical properties of stainless and structural steel dissimilar welds, 14 (2021) 6180.
- [7] M. K. Al Amin, I. Nurcholih, W. D. Pratiwi, D. Anggara, and E. W. RW, Comparative analysis of hardness and microstructure of dissimilar welded materials at various welding positions in the fabrication industry, 4 (2022) 1-8.
- [8] S. Haribabu, M. Cheepu, L. Tammineni, N. K. Gurasala, V. Devuri, and V. C. Kantumuchu, "Dissimilar friction welding of AISI 304 austenitic stainless steel and AISI D3 tool steel: Mechanical

- properties and microstructural characterization," in *Advances in Materials and Metallurgy: Select Proceedings of ICEMMM 2018*, 2019, pp. 271-281: Springer.
- [9] Cahyono, Analisis Radiografi Sinar-X Terhadap Sambungan Pelat Baja Tahan Karat Aisi 304 Hasil Pengelasan Tungsten Inert Gas Dengan Arus 40–60 Ampere, 6 (2021) 12-22.
- [10] A. Khalim, "Pengaruh Laju Aliran Gas Pada Pengelasan Tig Al 6061 Dan 5083 Terhadap Sifat Fisik Dan Mekanik," Universitas Muhammadiyah Ponorogo, 2023.
- [11] A. A. Rosidah, S. Suheni, and E. W. Anarki, "Analisis Pengaruh Diameter Elektroda dan Kecepatan Las terhadap Sifat Mekanik dan Struktur Makro pada Baja AISI 1050 dengan Proses Pengelasan TIG," in *Prosiding SENASTITAN: Seminar Nasional Teknologi Industri Berkelanjutan*, 2021, vol. 1, no. 1, pp. 408-414.
- [12] D. Mulyadi, R. A. Nanda, A. Abdulah, A. D. Shieddieque, and S. D. Prasetyo, "Box-Behnken Response Surface Methodology: An Analysis of the Effect of Variations in TIG Welding Parameters on TS loads and Hardness Using SUS 304 Material," in *Annales de Chimie. Science des Materiaux*, 2024, vol. 48, no. 3, p. 313: International Information and Engineering Technology Association (IETA).
- [13] M. Aissani, S. Guessasma, A. Zitouni, R. Hamzaoui, D. Bassir, and Y. Benkedda, Three-dimensional simulation of 304L steel TIG welding process: Contribution of the thermal flux, 89 (2015) 822-832.
- [14] B. Arivazhagan and M. Vasudevan, A comparative study on the effect of GTAW processes on the microstructure and mechanical properties of P91 steel weld joints, 16 (2014) 305-311.
- [15] B. Arivazhagan and M. Vasudevan, Studies on A-TIG welding of 2.25 Cr-1Mo (P22) steel, 18 (2015) 55-59.
- [16] K. H. Dhandha and V. Badheka, Effect of activating fluxes on weld bead morphology of P91 steel bead-on-plate welds by flux assisted tungsten inert gas welding process, 17 (2015) 48-57.
- [17] J. Liu, Z. Rao, S. Liao, and H.-L. Tsai, Numerical investigation of weld pool behaviors and ripple formation for a moving GTA welding under pulsed currents, 91 (2015) 990-1000.
- [18] A. Kumar, S. Maheshwari, and S. kumar Sharma, Optimization of Vickers hardness and impact strength of silica based fluxes for submerged arc welding by Taguchi Method, 2 (2015) 1092-1101.
- [19] EN 10025: 2019, Hot rolled products of structural steels - Part 2: Technical delivery conditions for non-alloy structural steels, 2019.
- [20] ASTM A283: 2018, Low and Intermediate TS loads Carbon Steel Plates, 2018.
- [21] ASTM A36: 1998, Standard Specification for Carbon Structural Steel, 1998.
- [22] JIS G3101: 2015, Rolled steels for general structure, 2015.
- [23] EN 10088-1: 1995, Stainless steels Part 1: List of stainless steels, 1995.
- [24] ASTM A240: 2023, Chromium and Chromium-Nickel Stainless Steel Plate, Sheet, and Strip for Pressure Vessels and for General Applications, 2023.
- [25] ASTM A276: 2023, Standard Specification for Stainless Steel Bars and Shapes, 2023.
- [26] DIN 17440:1996-09, Stainless steels - Technical delivery conditions for plates, hot rolled strip and bars for pressure purposes, drawn wire and forgings, 1996.
- [27] AWS A5.9: 2006, Specification for Bare Stainless Steel Welding Electrodes and Rods, American National Standard Institute: 2006.
- [28] ISO 14343: 2017, Welding consumables — Wire electrodes, strip electrodes, wires and rods for arc welding of stainless and heat resisting steels — Classification, 2017.
- [29] DIN 17100: 1980, Steel for General Structure Purposes, 1980.
- [30] ASTM A8: 2022, Standard Test Methods for Tension Testing of Metallic Materials, 2022.
- [31] M. Nofri, "Analisis ketangguhan antara baja st 37 dan st42 dengan ketebalan dan variasi lapisan karbon fiber untuk kerangka mobil listrik," ed: Presisi, 2019.
- [32] R. Wang *et al.*, Joining of 304 stainless steel to PET by semiconductor laser conduction welding, 27 (2023) 5729-5738.
- [33] H. Lin, C. J. S. Chou, T. o. Welding, and Joining, Optimisation of the GTA welding process using

- the Taguchi method and a neural network, 11 (2006) 120-126.
- [34] A. Thakur, V. J. A. J. f. S. Nandedkar, and Engineering, Optimization of the resistance spot welding process of galvanized steel sheet using the Taguchi method, 39 (2014) 1171-1176.
- [35] S. Sukarman *et al.*, Optimization of tensile-shear strength in the dissimilar joint of zn-coated steel and low carbon steel, 3 (2020) 115-125.
- [36] A. Basit *et al.*, Optimization of TIG welding parameters for tensile load testing on dissimilar material joints of galvanized steel (SGCC) and low carbon steel (SPCC-SD), 22 (2024) 378-382.